Corrosion Science 82 (2014) 173–179

Contents lists available at ScienceDirect

Corrosion Science

journal homepage: www.elsevier.com/locate/corsci

Eelectrochemical properties and corrosion resistance of carbon-ion-implanted magnesium

Ruizhen Xu, Xiongbo Yang, Penghui Li, Kai Wong Suen, Guosong Wu, Paul K. Chu *

Department of Physics and Materials Science, City University of Hong Kong, Tat Chee Avenue, Kowloon, Hong Kong, China

ARTICLE INFO

Article history:
Received 22 May 2013
Accepted 21 January 2014
Available online 30 January 2014

Keywords:
A. Magnesium
B. TEM
B. EIS
B. XPS
B. Ion implantation

ABSTRACT

The corrosion resistance of magnesium-based biomaterials is critical to clinical applications. In this work, carbon as a biocompatible and benign nonmetallic element with high chemical inertness is implanted into pure magnesium to improve the corrosion behavior. X-ray photoelectron spectroscopy (XPS), high-resolution transmission electron microscopy (HR-TEM), and Raman scattering reveal the formation of an amorphous carbon layer after ion implantation. Electrochemical studies demonstrate remarkable improvement in the corrosion resistance of magnesium in simulated body fluids (SBF) and Dulbecco's Modified Eagle Medium (DMEM).

1. Introduction

Magnesium and its alloys have mechanical properties that are more compatible with bone tissues than conventional biometals like stainless steels [1–3]. Furthermore, unlike passive metals such as titanium alloys and stainless steels, magnesium-based materials degrade spontaneously in the physiological environment thereby making implant removal after surgery unnecessary [4,5]. However, the degradation rate may be too fast to meet clinical needs, especially in the initial stage [6–8] and because the degradation procedure is dynamic, it is crucial to improve the surface corrosion resistance of magnesium and magnesium alloys.

Plasma immersion ion implantation (PIII) is an effective surface modification technique [9–11]. It has been shown that PIII enhances the biocompatibility and corrosion resistance enhancements of titanium alloys both *in vitro* and *in vivo* [12] and similar effects may be achieved on magnesium alloys. In fact, PIII of metallic ions including Al [13–15], Ti [14,16,17], Ta [18], Y [19], Ce [20], and Zr [14], gaseous ions such as N_2 [21], H_2O [22], O_2 [23], and H_2 [24]), and multiple ions including Cr–O [25,26] and Al–O [27]) have been proposed to suppress the fast degradation on magnesium and its alloys. In order to cater to clinical applications, the corrosion resistance of Mg must be improved while maintaining the surface biocompatibility as well as the mechanical characteristics after surface modification. Carbon has diverse structures and possesses beneficial chemical and physical properties such as high chemical inertness and tribological properties [28]. As a benign element to human beings, there are many carbon-based biomaterials with good biological properties, for instance, pyrolytic carbon [29,30] and diamond-like carbon [31,32]. Therefore, carbon ion implantation may be a good technique to enhance the corrosion resistance and biological characteristics of magnesium. In this work, carbon is plasma-implanted into magnesium and the surface properties and enhancement effects are investigated systematically.

2. Experimental details

The as-cast pure magnesium plate was cut into blocks with dimensions of $10\,mm \times 10\,mm \times 5\,mm$. The samples were mechanically polished by up to 1 μm alumina powder, ultrasonically cleaned in ethanol, and dried in air. Carbon ion implantation was carried out on an HEMII-80 ion implanter with a carbon cathodic arc source. The samples were implanted for 30 min at a terminal voltage of 20 kV and base pressure of 5×10^{-4} Pa.

Atomic force microscopy (AFM) was utilized to examine the morphology of the surface before and after carbon ion implantation. The surface mechanical properties were determined on an MTS nanoindentation instrument. Raman scattering was performed in air on a *LabRam HR* spectrometer (*Horiba Jobin Yvon*) equipped with an *Olympus BX41* microscope and an Ar^+ laser (green line at 2.41 eV or 514.5 nm). The elemental depth profiles and chemical states were determined by X-ray photoelectron spectroscopy (XPS, Physical Electronics PHI 5802). Al Kα irradiation was employed and the estimated sputtering rate was 6 nm min^{-1} based on a reference standard. The microstructure and composition were probed by high-resolution transmission electron microscopy (HRTEM, JEM-2010F) and energy-dispersive X-ray spectroscopy (EDS, Oxford INCA 200).

---

* Corresponding author.
E-mail address: paul.chu@cityu.edu.hk (P.K. Chu).

0010-938X/$ - see front matter © 2014 Elsevier Ltd. All rights reserved.
http://dx.doi.org/10.1016/j.corsci.2014.01.015

The electrochemical corrosion characteristics were evaluated on a Zahner Zennium electrochemical workstation based on the conventional three-electrode technique in simulated body fluids (SBF) [33] and Dulbecco's Modified Eagle Medium (DMEM, GIBCO, cat. no. 12100-046) [34] at 37 °C. The SBF solution containing inorganic ions with concentrations (in mM) similar to those in human extracellular fluids (142.0 Na^+, 5.0 K^+, 1.5 Mg^{2+}, 2.5 Ca^{2+}, 147.8 Cl^-, 4.2 HCO_3^-, 1.0 HPO_4^{2-}, 0.5 SO_4^{2-} with a pH of 7.40) was prepared by dissolving reagent grade (in mM) 137.4914 NaCl, 4.2258 $NaHCO_3$, 3.0181 KCl, 1.0122 $K_2HPO_4 \cdot 3H_2O$, 1.5297 $MgCl_2 \cdot 6H_2O$, 2.6311 $CaCl_2$, and 0.5068 Na_2SO_4 in distilled water and buffered at pH 7.4 with 50.5035 mM trishydroxymethyl aminomethane (TRIS) and 1.0 M HCl. The DMEM cell culture medium was prepared by DMEM powder and the constituents were (in mM): 0.4 glycine, 0.39810428 L-arginine hydrochloride, 0.20127796 L-cystine 2HCl, 4 L-glutamine, 0.2 L-histidine hydrochloride·H_2O, 0.8015267 L-isoleucine, 0.8015267 L-leucine, 0.7978142 L-Lysine hydrochloride, 0.20134228 L-methionine, 0.4 L-phenylalanine, 0.4 L-serine, 0.79831934 L-threonine, 0.078431375 L-tryptophan, 0.39846742 L-tyrosine disodium salt dihydrate, 0.8034188 L-valine, 0.028571429 choline chloride, 0.008385744 D-calcium pantothenate, 0.009070295 folic Acid, 0.032786883 niacinamide, 0.019607844 pyridoxine hydrochloride, 0.00106383 riboflavin, 0.011869436 thiamine hydrochloride, 0.04 i-inositol, 1.8018018 $CaCl_2$, 2.48×10^{-4} $Fe(NO_3)_3 \cdot 9H_2O$, 0.8139166 $MgSO_4$, 5.3333335 KCl, 110.344826 NaCl, 0.9057971 $NaH_2PO_4 \cdot H_2O$, 25 dextrose, and 0.039851222 phenol red. The potential was referenced to a saturated calomel electrode (SCE) and the counter electrode was a platinum sheet. The working electrode was mounted with silicone to expose an area of 10 mm × 10 mm. The EIS data were collected from 100 kHz to 100 mHz with a 5 mV sinusoidal perturbation signal. The polarization curves were acquired at a scanning rate 2 mV s^{-1} right after the EIS tests and the corrosion morphologies after the electrochemical tests were examined by scanning electron microscopy (SEM, FEI/Philips XL30 Esem-FEG).

3. Results and discussion

The atomic force microscopy (AFM) images of the untreated Mg and carbon-implanted Mg in Fig. 1 are quite different. The untreated sample has uniformly distributed and small cones with scratches produced during mechanical polishing (Fig. 1a). On the other hand, Fig. 1b shows that the surface of carbon–implanted Mg has large dome shaped islands and more distinguished scratches. The root-mean-square (RMS) roughness values of the untreated Mg and treated Mg are 6.43 and 5.15 nm, respectively. A smoother surface was obtained after ion implantation probably due to surface restructuring at elevated temperature during implantation [11,35].

As shown in Fig. 2, there are no significant changes in the hardness and elastic modulus between the implanted and unimplanted samples. The reproducibility of the nanoindentation measurements is determined by repeating the tests four times and the error bar represents one standard deviation. The modulus after carbon ion implantation increases from 36 GPa to 40 GPa but the hardness diminishes slightly from 0.64 GPa to 0.52 GPa. Although higher hardness has been reported from DLC coatings [36], our data disclose that the hardness and modulus after implantation are similar to those of the unimplanted sample. The results are actually quite desirable because the favorable surface mechanical properties of magnesium are maintained after carbon PIII.

The Raman scattering spectra acquired from the carbon–implanted magnesium in Fig. 3 shows the typical pattern of amorphous carbon (a-C films). The most common Raman spectra fitting method is to employ two Gaussian peaks with linear background subtraction with the G peak centered at around 1540–1580 cm^{-1} and D peak centered around 1350 cm^{-1} [36]. It is based on the assumption that the amorphous carbon films are composed of sp^2 and sp^3 networks. In this study, the Raman spectrum can be deconvoluted into two sub-peaks: G peak at 1554.4 cm^{-1} and D peak at 1381.9 cm^{-1}. Similar Raman spectra have been obtained from DLC coatings on Mg alloys [36,37]. The D peak can be ascribed to the evolution to nano-crystalline graphite accompanied by conversion of sp^3 bonds to sp^2 bonds [37].

The XPS depth profiles obtained from the implanted sample is depicted in Fig. 4. The concentrations of carbon, magnesium, and oxygen, change gradually with depth in the implanted sample. The surface oxygen stems from surface contamination and spontaneously oxidation due to the non-ultra-high-vacuum (UHV) conditions [28]. The carbon concentration drops quickly from 80% initially to about 10% after sputtering for 4 min and the low C concentration diminishes slowly throughout a depth of about 34 nm. The carbon-containing layer is therefore inferred to be about 58 nm thick.

The common chemical bonds in amorphous and nanocrystalline carbon are sp^3 and sp^2 hybridizations and XPS can reveal the C binding energy and discern the sp^3 and sp^2 bonds. In the sp^3 configuration, a carbon atom forms four sp^3 orbitals and makes a strong σ bond to the adjacent atom. In the sp^2 configuration, a carbon atom forms three sp^2 orbitals and forms three σ bonds and the remaining p orbital forms a π bond. Fig. 5a depicts the C 1s spectra at different sputtering time showing the C 1s peak has both sp^2 and sp^3 components. The peak at a binding energy of 284.3 eV is attributed to sp^2 carbon atoms whereas that 285.3 eV is due to sp^3 carbon atoms. A large sp^3 content in excess of 80% is associated with high hardness [11]. In our samples, owing to relatively small sp^3 content, the hardness before and after carbon ion implantation does not change much. The high fraction of sp^2

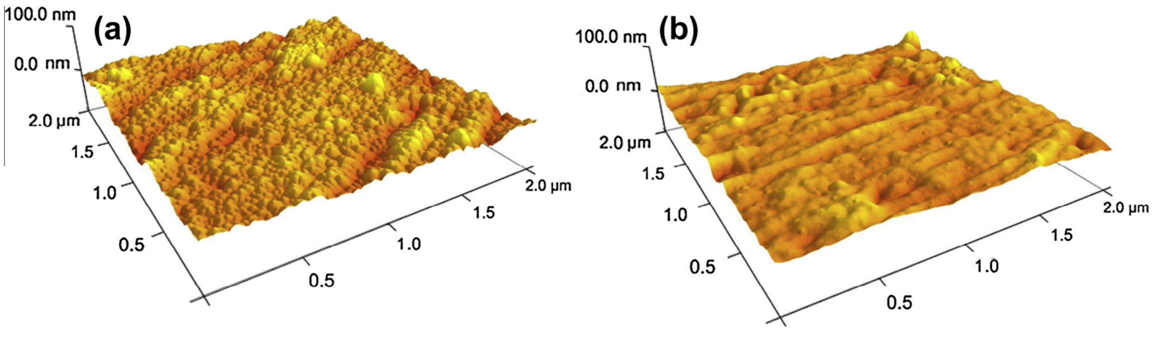

Fig. 1. Surface morphologies obtained by atomic force microscopy (AFM): (a) untreated Mg and (b) carbon-implanted Mg.